TRPML1-mediated Modulation of Dense-core Granules Tunes Functional Potential in NK Cells

Jodie P. Goodridge[1,2], Benedikt Jacobs[1,2], Michelle L. Saetersmoen[1,2], Dennis Clement[1,2], Trevor Clancy[1,2], Ellen Skarpen[3], Andreas Brech[3], Johannes Landskron[1,4], Christian Grimm[5], Aline Pfefferle[6], Leonardo Meza-Zepeda[7,8], Susanne Lorenz[8], Merete Thune Wiiger[1,2], William E. Louch[9], Eivind Heggernes Ask[1,2], Lisa L. Liu[6], Vincent Yi Sheng Oei[1,2], Una Kjällquist[10], Sten Linnarsson[10], Sandip Patel[11], Kjetil Taskén[1, 2, 4], Harald Stenmark[3], Karl-Johan Malmberg[1,2,6]

Inhibitory signaling during natural killer (NK) cell education translates into increased responsiveness to activation; however the intracellular basis for functional tuning by inhibitory receptors remains unclear. We found that NK cells expressing self-MHC specific inhibitory killer cell immunoglobulin -like receptors (KIR) show a greater accumulation of dense-core secretory granules, converged closer to the centrosome in resting NK cells, which are released upon recognition of target cells. This discrete morphological phenotype persists in self-KIR+ NK cells independently of transcriptional programs that regulate metabolism and granule biogenesis and indicates an intrinsic role for lysosomal homeostasis in NK cell education. Upon activation, interference of signaling from acidic Ca^{2+} stores reduced both target-specific Ca^{2+}-flux, degranulation and cytokine production. Furthermore, inhibition of PI(3,5)P2 synthesis or genetic silencing of the PI(3,5)P2-regulated lysosomal Ca^{2+}-channel TRPML1 in primary NK cells led to an increase in granular load and enhanced functional potential. These results suggest a model where continuous unopposed signaling through activating receptors render NK cells hypofunctional through TRPML1-mediated modulation of acidic Ca^{2+} stores.

Natural killer (NK) cells achieve specificity through unique combinations of variable germ-line encoded receptors. These receptors are critical for the development of cell-intrinsic functional potential, which enables spontaneous activation upon recognition of target cells displaying reduced class I MHC expression.[1].Inhibitory interactions with self-MHC translate into a predictable quantitative relationship between self-recognition and effector potential, a process termed NK cell education.[2] Despite being clearly evident in different species,[3] NK cell education operates through an as yet largely unknown mechanism. Paradoxically, mature NK cells expressing self-MHC specific inhibitory receptors, receiving constitutive inhibitory input, exhibit increased levels of functionality. Mouse models have demonstrated that this functional phenotype is dynamic and dependent on the net signaling input to NK cells during cell-to-cell interactions both with stromal and hematopoietic cells[4]. Transfer of mature NK cells from one MHC environment to another results in reshaping of the functional potential based on the inhibitory input of the new MHC setting.[5] Alternatively, genetic knockdown of SLAM-family receptors by CRISPR/Cas9 leads to hyperfunctionality,[6] whereas deletion of the inhibitory signaling through ITIM and SHP-1 renders NK cells hypofunctional.[7, 8] However, it remains unclear how and when the net signaling input from activating and inhibitory receptors during NK cell education tune the functional potential of the cell. One difficulty in establishing the cellular and molecular mechanisms that account for the calibration of NK cell function is the lack of a steady-state phenotype that defines the educated NK-cell state. Functional readouts used to distinguish self-specific NK cells from hyporesponsive NK cells do not provide information about the prior events that culminate in the development of effector potential. Apart from differences in the relative levels and distribution of NK cell receptors at the cell membrane,[9, 10] transcriptional and phenotypic readouts at steady state provide scant differences between self and non-self specific NK cells.[11, 12] While the confinement of activating receptors to areas that are permissive for signaling holds important clues

[1]The KG Jebsen Center for Cancer Immunotherapy, Institute of Clinical Medicine, University of Oslo, 0318 Oslo, Norway. [2]Department of Cancer Immunology, Institute for Cancer Research, Oslo University Hospital, 0310 Oslo, Norway. [3]Department of Molecular Cell Biology, Institute for Cancer Research, Oslo University Hospital, 0310 Oslo, Norway. [4]Centre for Molecular Medicine Norway, Nordic EMBL Partnership, University of Oslo and Oslo University Hospital, 0318 Oslo, Norway. [5]Department of Pharmacy, Center for Drug Research, Ludwig-Maximilians-Universität München, Germany. [6]Center for Infectious Medicine, Department of Medicine Huddinge, Karolinska Institutet, 14186 Stockholm, Sweden. [7]Department of Tumor Biology, Institute for Cancer Research, The Norwegian Radium Hospital, Oslo University Hospital, Oslo, Norway. [8]Genomics Core Facility, Department of Core Facilities, Institute for Cancer Research, The Norwegian Radium Hospital, Oslo University Hospital, Oslo, Norway. [9]Institute for Experimental Medical Research, Oslo University Hospital and University of Oslo, 0424 Oslo, Norway. [10]Division of Molecular Neurobiology, Department of Medical Biochemistry and Biophysics, Karolinska Institutet, S-17177 Stockholm, Sweden. 11Department of Cell and Developmental Biology, University College London, Gower Street, London WC1E 6BT, UK.

for the increased reactivity of self-specific NK cells, precisely how these structural changes translate into a profound difference in functionality between self and non-self specific NK cells remains to be established. The critical question is whether qualitative differences in proximal receptor signaling alone explains NK cell education or whether the functional potential of the cell can be a linked to a cellular mechanism that develops prior to target cell recognition as the cell interacts with its microenvironment. Whether inhibitory signalling leads to gain of function through an as yet unknown mechanism, a concept referred to as arming/stimulatory licensing, or that inhibitory receptors simply tune out tonic activation that would otherwise lead to erosion of function over time (e.g. disarming/inhibitory licensing)[3, 13, 14] remains to be determined. Priming of NK cell effector function, in both mouse and human, depends on homeostatic cytokines, including IL-15 and type I interferon[15, 16, 17], and is affected by metabolic cues[18, 19]. Under germ-free conditions, animal models of acute infection result in a tidal upregulation of the transcription of effector loci in NK cells, which resolve with normal immune kinetics[20]. In humans, the full cumulative spectrum of NK cell differentiation is determined epigenetically and revealed through graded increases in the cellular content of both granzyme B and perforin, coupled to increasing capacity for both cytolysis and cytokine production[21]. Here we sought to examine how priming, granular development and receptor-mediated in-

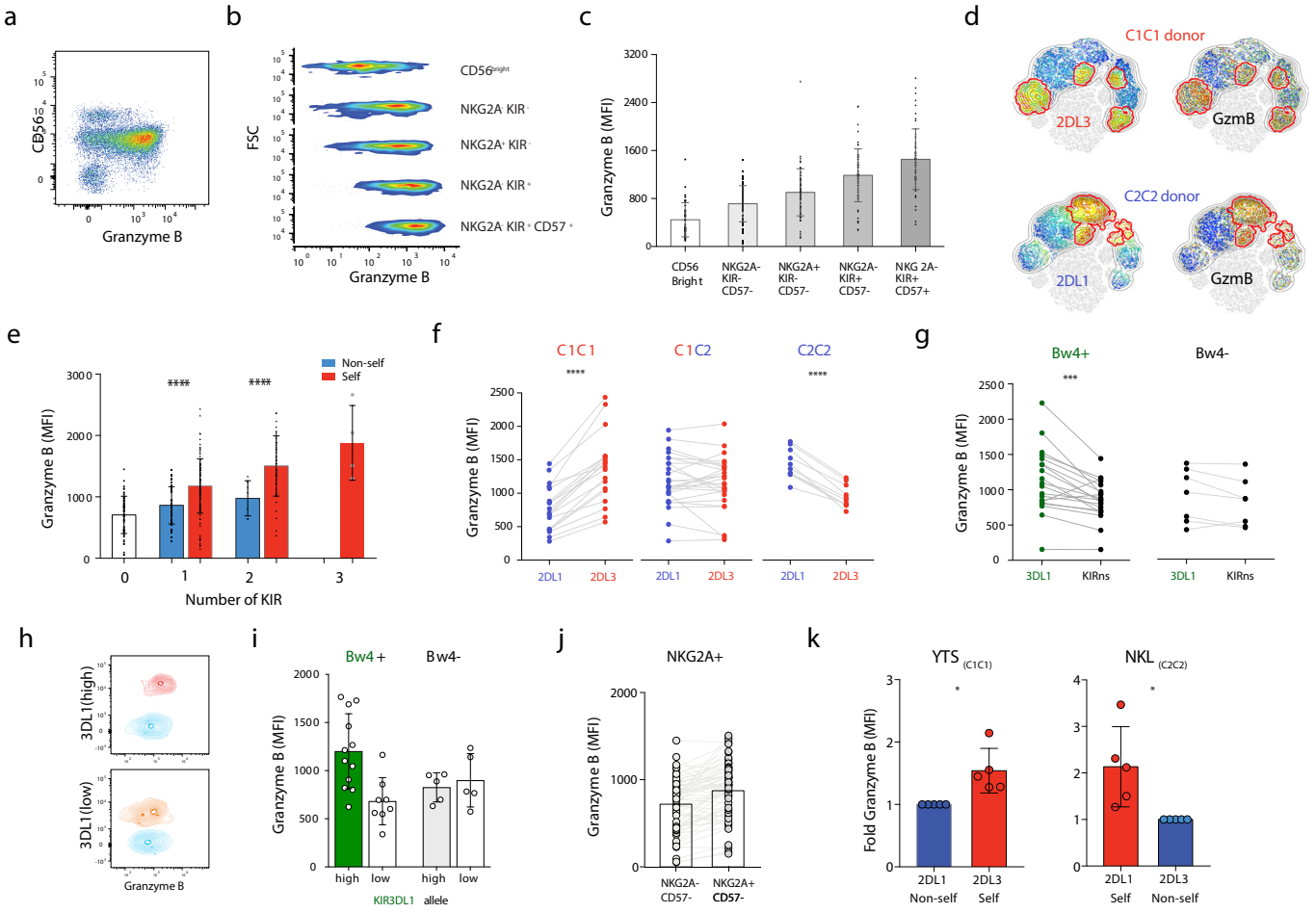

Figure 1. Self-recognition is associated with increasing granular load in primary resting NK cells. (a-c) Expression of granzyme B in the indicated NK cell subsets. (d) SNE plot showing intensity of granzyme B in clusters defined by 2DL3 and 2DL1 expression in C1/C1 and C2/C2 donors, respectively. (e) Expression of granzyme B in subsets of NK cells expressing 0, 1-2 Non-Self or 1-3 Self KIR. (f) Expression of granzyme B in 2DL3 and 2DL1 single-positive NK cells from C1/C1, C1/C2 and C2/C2 donors. (g) Expression of granzyme B in 3DL1+/- NK cells from Bw4+ and Bw4- donors. (h-i) Expression of granzyme B in 3DL1high and 3DL1low NK cells from Bw4+ and Bw4- donors. (j) Expression of granzyme B in NKG2A+KIR-CD57- versus NKG2A-KIR-CD57- NK cells. (k) Expression of granzyme B in YTS and NKL cells transfected with 2DL3 or 2DL1.

hibition are coordinated to establish and maintain a steady state functional potential in mature NK cells. Our findings suggest that inhibitory receptors oppose TRPML1-mediated disarming through modulation of the lysosomal pathway, including the secretory granules. Hence, NK cells expressing self-specific KIR effectively sequester functional potential through manipulation of the endolysosomal compartment, allowing them to subsequently mount strong, spontaneous effector responses from pre-existing granular stores. Moreover, the granular compartment itself appears to contribute to Ca^{2+}-flux and distal signaling, effectively connecting homeostatic receptor input to lysosomal homeostasis in order to determine the enhanced functional potential observed in self-KIR+ NK cells.

RESULTS

Self-recognition is associated with increasing granular load in primary resting NK cells

In order to address the possible mechanisms involved in tuning of effector potential, the expression of cytotoxic effector molecules was monitored in resting NK cells by flow cytometry in discrete subsets corresponding to different stages of differentiation, from $CD56^{bright}$ NK cells through subsets of mature $CD56^{dim}$ NK cells defined by the expression of NKG2A, KIR and CD57.[22] The expression of cytolytic effector molecules granzyme B and perforin increased gradually, whereas granulysin decreased, as NK cells became more differentiated. (Fig. 1a-c and Supplementary Fig. 1a). Next, granzyme B content in mature NK cells was stratified based on the expression of self versus non-self specific KIR. The stochastic expression of KIR in NK cells is independent of the MHC setting and provides a unique and natural equivalent of in vivo gene-silencing.[23, 24] This allowed us to address the impact of reciprocal presence or absence of a self-KIR on granular content between individuals. Clustering of NK cell phenotypes using t-distributed stochastic neighbor embedding (tSNE) revealed high expression of granzyme B in NK cell subsets expressing self-specific KIR (Fig. 1d). Extended analysis of 64 healthy donors showed significantly higher expression of granzyme B in NK cells expressing one or more self-specific KIR in donors homozygous for HLA-C1/C1 or HLA-C2/C2, ligands for KIR2DL3 (2DL3) and 2DL1, respectively, in NK cells that were NKG2A negative and CD57 negative, in order to control for the stage of differentiation (Fig. 1e, f). Similar trends were observed for perforin and granulysin that were both expressed at higher levels in self-specific NK cells (Supplementary Fig. 1b). Corroborating the link between inhibitory input through self-KIR and granzyme B expression, donors that were heterozygous for HLA-C1/C2 had similarly high levels of granzyme B in both 2DL1 and 2DL3 single-positive NK cells (Fig. 1f). Granzyme B expression was also higher in 3DL1+ NK cells from donors positive for its cognate ligand HLA-Bw4 (Fig. 1g) and varied according to the expression level of 3DL1 (Fig. 1h). NK cells with higher levels of 3DL1 surface expression, also known to have a higher functional capacity,[25] exhibited greater expression of granzyme B. Notably, this phenomenon was only observed in the presence of its cognate ligand in HLA-Bw4+ donors (Fig. 1i). It is well established that NKG2A/HLA-E interactions contribute to education of NK cells.[26, 27, 28] In line with the results of single KIR+ NK cell subsets, NKG2A+KIR-CD57- NK cells expressed higher levels granzyme B (Fig. 1j). To study the effect of self KIR expression in a dynamic model, retroviral transduction was used to introduce full length 2DL1 or 2DL3 into NK cell lines YTS (HLA-C1/C1) and NKL (HLA-C2/C2). Corroborating the findings with ex vivo staining of primary NK cells, the transduced NK cell lines showed a similar accumulation of granzyme B following transfection of a self KIR (Fig. 1k) and enhanced functionality (Supplementary Fig. 1c-d). These data show that the expression of inhibitory self-KIR or NKG2A are connected to the granular load of an NK cell, establishing a link between inhibitory input and the regulation of the core cytolytic machinery of NK cells.

Inhibitory input influences the level of granular content independently of transcriptional cell differentiation programs

To address whether the increased levels of granzyme B in educated NK cells were due to gene expression, we first examined the transcriptional regulation of effector programs within the context of NK cell differentiation. Transcriptome analysis was performed using single-cell tagged reverse transcription (STRT),

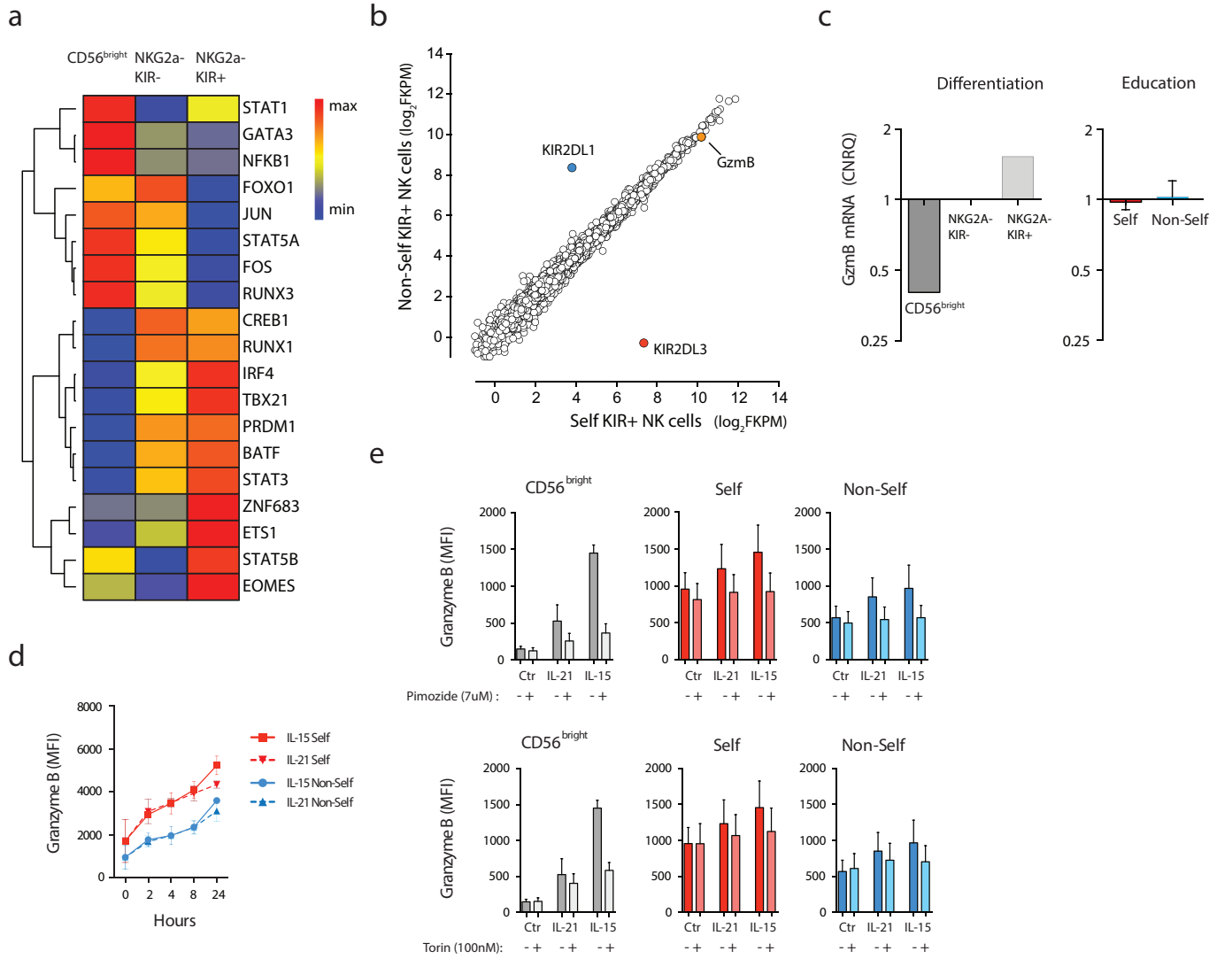

Figure 2 Inhibitory input influences the level of granular content independently of transcriptional cell differentiation programs (a) mRNA expression (RNA-Seq) of the indicated genes in CD56^{bright}, NKG2A-KIR- and NKG2A-KIR+ CD56^{dim} NK cell subsets. (b) Global RNA-Seq and (c) quantitative PCR of granzyme B mRNA (bottom) in the indicated NK cell subsets. (d) Expression of granzyme B in the indicated NK cell subsets following stimulation with IL-15 or IL-21 for the indicated length of time. (e) Expression of granzyme B after 24h of stimulation with IL-21 or IL-15 in the indicated NK cell subset in the presence or absence of the STAT-5 inhibitor Pimozide (top) (7μM) and the mTOR inhibitor Torin-1 (100nM) (bottom).

a highly multiplexed method for single-cell RNA sequencing (RNA-Seq).[29] Naïve CD56^{bright} NK cells and five CD56^{dim} NK cell subsets, sorted on the expression of NKG2A and KIR were analysed. Since the exact order of transitions between intermediate stages of CD56^{dim} NK cell differentiation is not known, we focused our analysis on three discrete subsets representing previously defined stages of NK cell differentiation: CD56^{bright}, CD56^{dim} NKG2A-KIR- and CD56^{dim} NKG2A-KIR+ NK cells.[22] Analysis of transcription factors linked to the regulation of GzmB revealed that the immature CD56^{bright} NK cells predominantly expressed higher levels of transcription factors associated with responsiveness to acute stimulation such as AP1, STAT-1, STAT-5 and NF-kB. The more mature CD56^{dim} NK cell subsets, on the other hand, expressed higher levels of transcription factors associated with cellular differentiation, including TBX21 and PRDM1, and maintenance of effector expression, such as BATF, IRF4, and NFATc1[30, 31, 32] (Fig. 2a). Within the context of differentiation, levels of IRF4 correlated closely with granzyme B expression

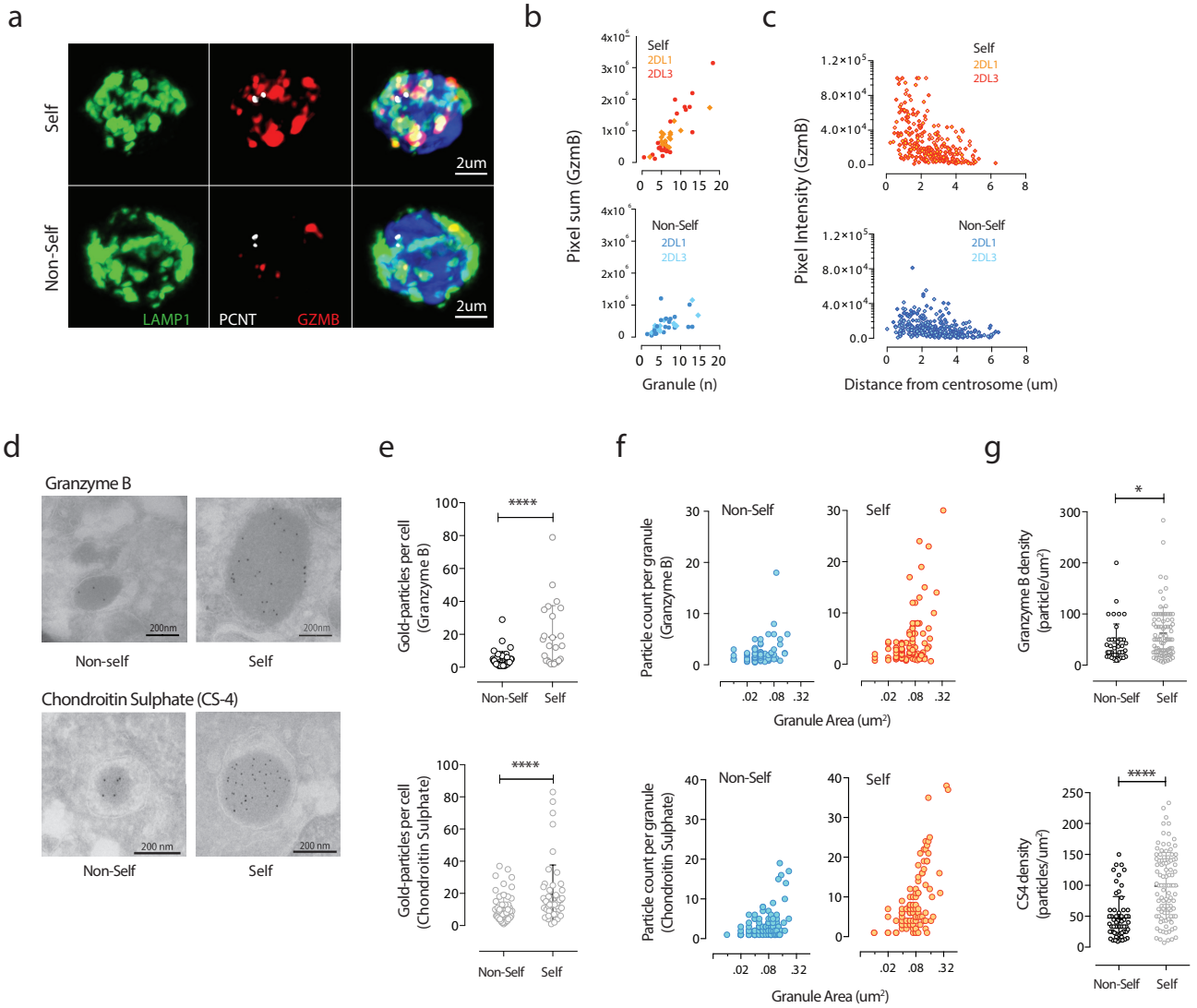

Figure 3 Accumulation of converged dense-core secretory granules in self-KIR+ NK cells (a) Representative confocal microscopy Z-stack showing Pericentrin (PCNT), LAMP-1 and granzyme B (GZMB) staining in sorted CD56^{dim} NKG2A-CD57- NK cells expressing Non-Self or Self KIR. (b) The pixel sum of granzyme B staining in cells expressing Non-Self (bottom) or Self KIR (top) versus the number of granules. Data are aggregated from sorted 2DL1 and 2DL3 single-positive NK cell subsets from C1C1 (n=3-5) and C2C2 (n=2-5) donors. (c) Granzyme B expression levels in individual granules in NK cells expressing Non-Self or Self KIR versus the distance from the centrosome. (d) Representative immuno-EM image showing staining with gold-particle coated anti-granzyme B (top) and chondroitin Sulphate-4 (CS-4) (bottom) staining of sorted CD56^{dim} NKG2A-CD57- NK cells expressing Non-Self or Self KIR. (e) Number of gold particles (granzyme B and CS-4) per cell. (Non-Self n=83, Self n=109). (f) Particle count (granzyme B and CS-4) as a function of the granular area. (g) Density of gold particles (granzyme B and CS-4) per granule area (μm2).

at both the transcript and protein level (Supplementary Fig. 2a-b) Although there is limited data on their role in human NK cell differentiation, TBX21, PRDM1 and IRF4 have been previously associated with transcription of GzmB, Prf1 and IFNG.[30, 33] Next, we addressed whether the transcriptional changes associated with NK cell differentiation and KIR acquisition accounted for the observed differences in granzyme B content between self and non-self specific NK cell subsets. NKG2A-CD57- NK cells were sorted by FACS into 2DL3 or 2DL1 single positive populations from C1/C1 and C2/C2 donors and transcriptionally profiled using RNA-Seq. In line with previous studies in mice,[9] there was a near perfect correlation between genes expressed in educated and hyporesponsive human NK cell subsets, including genes encoding transcription factors for effector loci, granule biogenesis, and mechanistic target of rapamycin (mTOR) regulated metabolism (Fig. 2b). These results were confirmed in a panel of 20 selected qPCR targets comprising transcription factors and canonical cell surface markers linked to NK cell differentiation, GzmB regulation

and granule biogenesis (Supplementary Fig. 2c and Supplementary Table 1). Notably, we found no difference in granzyme B mRNA expression between the sorted self and non-self specific NK cell subsets (Fig. 2c) or between NKG2A+ and NKG2A- NK cells (Supplementary Fig. 2d). These data demonstrated that the increased levels of effector molecules such as granzyme B detected by flow cytometry in self-KIR+ NK cells occur independently of transcriptionally regulated programs, including differences in tonic metabolic input to the cell, at least at the level of gene expression. In mouse NK cells, expression of granzyme B is further regulated by cytokine-induced translation from a preexisting pool of mRNA transcript.[15] Therefore, we explored the possibility that self and non-self specific NK cells may respond differentially to cytokine priming in vivo, resulting in divergent steady-state levels of expressed granzyme B. To address this possibility, NK cells exposed to IL-15 or IL-21 for various lengths of time were monitored for granzyme B content using flow cytometry (Fig. 2d). Both self and non-self KIR+ CD56^{dim} NK cells displayed increased levels of granzyme B in response to IL-15 and IL-21 stimulation. Notably, the relative differences in granzyme B between self and non-self specific NKG2A-CD57- NK cells were similar after stimulation with IL-15 or IL-21 (Fig. 2d). Furthermore, blockade of STAT-5 and mTOR signaling with Pimozide and Torin-1, respectively, abolished the cytokine-induced increase in granzyme B in both self and non-self specific NK cells (Fig. 2e). Importantly, the same treatment with Pimozide and Torin-1 did not further reduce the pre-existing constitutive levels of granzyme B that preceded cytokine stimulation. Similar effects were noted with the Janus kinase inhibitor Ruxolitinib and the STAT3 inhibitor S3I-201 (Supplementary Fig. 3a). Furthermore, no differences were observed in the global levels of LAMP1 (Supplementary Fig. 3b), suggesting that active lysosomal biogenesis, known to be driven by TFEB, also did not account for the differences in granzyme B content. Similar to stimulation with cytokines, the rate at which lysosomal biogenesis was induced by starvation was equivalent in self and non-self specific NK cells (Supplementary Fig 3c-d). These data indicate that the observed differences in granzyme B levels at rest are stable and refractory to interference of either STAT or mTOR signaling, suggesting that a stable pool of granzyme B is retained by NK cells independently of constitutive input through cytokine or metabolic signals.

Accumulation of converged dense-core secretory granules in self-KIR+ NK cells The finding that self-KIR+ NK cells expressed higher levels of granzyme B independently of gene expression provided an initial insight into possible post-transcriptional mechanisms underlying the increased functional potential associated with NK cell education. Granzyme B is sequestered into granular structures within the acidic compartment of the cell. To determine whether the increased levels of granzyme B in self-specific NK cells was a result of higher density, number, or size of cytolytic granules, or a combination thereof, NKG2A-CD57- NK cell subsets were sorted ex vivo into self- or non-self specific NK cell subsets and imaged by confocal microscopy. Corroborating the difference in granzyme B expression observed using flow cytometry, self-KIR+ NK cells had a higher overall intensity of granzyme B staining, localized within granular structures (Fig. 3a and Supplementary Fig. 4a). The average number of granzyme B containing granules, as defined by discrete points of localized staining intensity, was similar between self and non-self specific NK cells. However, self-KIR+ NK cells displayed an increased level of fluorescence intensity for granzyme B in the granular areas (Fig. 3b), which in turn correlated with proximity to the centrosome (Fig. 3c). Optical resolution limits of confocal microscopy prevented accurate assessment of granule size and determination of areas with high granzyme B intensity. To address more precisely the size and density of individual granules, sorted self-KIR+ and non-self KIR+ NK cells were sectioned and stained for immuno-electron microscopy (Immuno-EM) using anti-granzyme B mAb and Protein A-gold (Fig. 3d). Quantification of gold particles per cellular section revealed overall greater granzyme B staining in educated NK cells, consistent with both the flow cytometry and confocal microscopy (Fig. 3d-e). Since retention of granzyme B and re-loading of granules depends on the serglycin content in the granular matrix,34 sections of self-KIR+ and non-self KIR+ NK cells were stained for expression of Chondroitin Sulphate 4 (CS4), a predominant glycosaminoglycan side-chain associated with serglycin in cytotoxic lymphocytes.[35] Self-KIR+ NK cells had a higher overall intensity of CS4-staining (Fig. 3d-e), suggesting that inhibitory interactions with self-MHC may influence the accumulation of the granular ma-

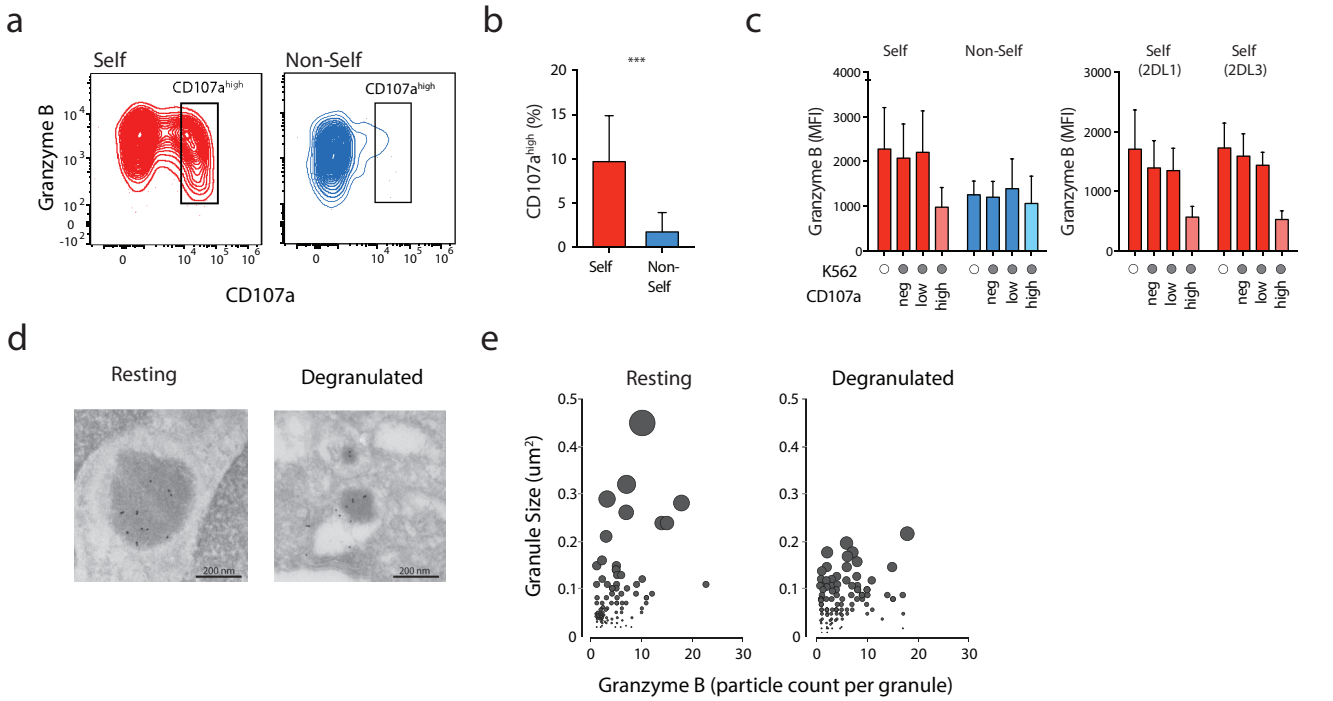

Figure 4. Self-KIR+ NK cells release large dense-core granules and mobilize granzyme B down to base-line levels following target cell stimulation (a) Representative example of granzyme B and CD107a expression in Self KIR+ and Non-Self KIR+ CD56^{dim} NKG2A-CD57- NK cells following stimulation with K562 cells. (b) Aggregated data of percent CD107a^{high} NK cells following stimulation with K562 cells (n=5). (c) Expression of granzyme B in the indicated NK cell subset after stimulation with K562. Left graph: C1/C1 donors (n=4), Right graph: C1/C2 donors (n=4). (d) Representative Immuno-EM image of resting or sorted CD107a^{high} NK cells. (e) Granular size and granzyme B content as determined by immuno-EM in resting and sorted CD107a^{high} NK cells after stimulation with K562.

trix. Granzyme B and CS4 staining further revealed a small increase in the average granular size, resulting in a larger total granular area, without significant difference in relative cell size (Supplementary Fig. 4b-d). Similarly, analysis of gold particle distribution against granular area in immuno-EM images revealed that self-specific NK cells had larger granzyme B-dense granule areas (Fig. 3f), and overall greater granule densities (Fig. 3g). These data provide a link between expression of self-specific inhibitory KIR and retention of enlarged, granzyme B-dense cytotoxic granules.

Self-KIR+ NK cells mobilize large dense-core granules and release granzyme B to levels of non-self-KIR+ following target cell stimulation Recent evidence suggests that the actin meshwork provides physical constraint on the release of secretory granules over a certain size.[36] Therefore, we examined the fate of dense-core granules relative to size following stimulation with K562 cells. Granzyme B release in self KIR+ NK cells was associated with strong granule mobilization, reflected in a higher discrete mode of CD107a expression (CD107a^{high}) (Fig. 4a-b), and accompanied by a decrease in granzyme B expression to the levels observed in non-self specific KIR+ NK cells (Fig. 4c). Immuno-EM of sorted CD107a^{high} NK cells revealed a specific reduction of large and granzyme B-dense granules following target cell interaction (Fig. 4d-e). Thus, the accumulation of dense-core granules during education and their effective release upon stimulation, provide a plausible explanation for the enhanced cytotoxic potential of self-KIR+ NK cells.

Role of the acidic Ca^{2+} stores in determining functional potential in NK cells Given that the secretory granules in killer cells share common features with the lysosomal compartment, including the maintenance of low pH and markers of lysosomes, we next set out to examine whether the increase in dense-core granules in educated NK cells was affected by regulation of lysosomal activity and whether this has further consequences for global responses to receptor ligation. Given the qualitative differences in the lysosomal compartments in self-KIR+ versus nonself-KIR+ NK cells with respect to granularity, lysosomal Ca^{2+} signaling was examined to gauge the relative capacity of the acid-

ic compartment, including the secretory granules, in terms of uptake and release of intracellular Ca^{2+} since this bears important implications for NK cell functions including exocytosis[37] and cytokine production.[38] Functional responses of primary NK cells were determined in the presence and absence of glycyl-L-phenylalanine-beta-naphthylamide (GPN), a dipeptide substrate of cathepsin-C associated with release of Ca^{2+} from the lysosomes.[39] GPN causes osmotic permeablization of cathepsin C-positive compartments 40, resulting in the collapse of the pH gradient and controlled equilibration of small solutes (dictated by donnan equilibrium), including Ca^{2+}, between the acidic compartment and the cytosol.[39] Treatment of resting primary NK cells with GPN dampened the detection of global Ca^{2+}-flux in the cytosol in response to ligation with CD16 or a combination of DNAM-1 and 2B4 (Fig. 5a). GPN treatment alone resulted in a low level of mobilization of CD107a+ vesicles to the cell surface (Fig. 5b) but abrogated degranulation and more importantly abrogated the production of IFNγ in response to K562 cells (Fig. 5b-c). Similar results were obtained using mefloquine, another lysosomotropic agent that specifically disrupts lysosomal homeostasis through buffering of the acidic pH gradient[41, 42] (Fig. 5d). Thus, disruption of the lysosomal compartment not only affects the mobilization of secretory granules but also the production of cytokines, suggesting that cytokine production in response to stimuli requires lysosomal-derived signals. This opens the possibility that differential signalling in self-KIR+ and nonself-KIR+ NK cells may be influenced by lysosomal-derived Ca^{2+} signals. Importantly, none of these compounds showed any general cellular toxicity at the doses tested as compared to the positive control L-Leucyl-L-leucine methyl ester (LeuLeuOMe), a lysosomotropic agent known to induce apoptosis in immune cells through induced lysis of cytotoxic granules (Supplementary Fig. 5). Furthermore, GPN treatment did not interfere with degranulation in response to PMA/Ionomycin, which raises cytosolic free Ca^{2+} by directly accessing both intra- and extra-cellular free Ca^{2+}. In fact, degranulation in response to treatment with PMA/Ionomycin was inversely correlated with the granzyme B content of the cell (Supplementary Fig. 6a-c). Ionomycin does not work against an acidic pH gradient,[43] thus disruption of the lysosomal compartment with GPN rescued PMA/Ionomycin-induced degranulation in differentiated and self-KIR+ NK cells (Supplementary Fig. 6d-e). The effects of disrupting the pH and donnan potential of the acidic compartment, which contains the cytolytic granules, support a role for the acidic compartment in modulating the flow of free-cytosolic Ca^{2+}, and corroborate the notion that secretory granule may contribute to the tuning of effector responses in NK cells.

Pharmacological inhibition of $PI(3,5)P_2$ synthesis leads to formation of large secretory granules and enhanced NK cell functionality The lysosomal compartment undergoes constant modulation through Ca^{2+} regulated fission and fusion events.[44, 45]

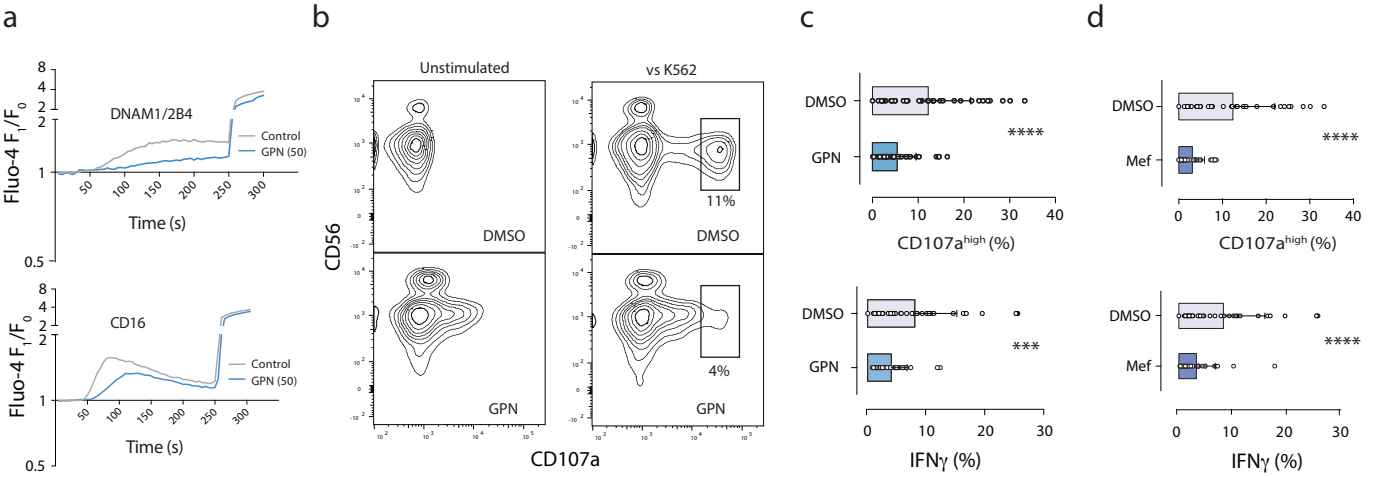

Figure 5. Role of the secretory granule in determining activation thresholds in NK cells (a) Global Ca^{2+}-flux measured by Fluo-4 F1/F0 ratio following stimulation with biotinylated anti-DNAM-1/anti-2B4 (top) or biotinylated anti-CD16 (bottom) crosslinked with streptavidin in the presence of absence of GPN (50μM). (b) Representative example of granzyme B and CD107a expression following stimulation of NK cells with K562 cells in the presence or absence of GPN. Frequency of $CD107^{high}$+ (top) and IFN-γ+ (bottom) NK cells following stimulation with K562 cells in the presence or absence of (c) 50uM GPN (n=32) and (d) 10uM Mefloquine (n=32).

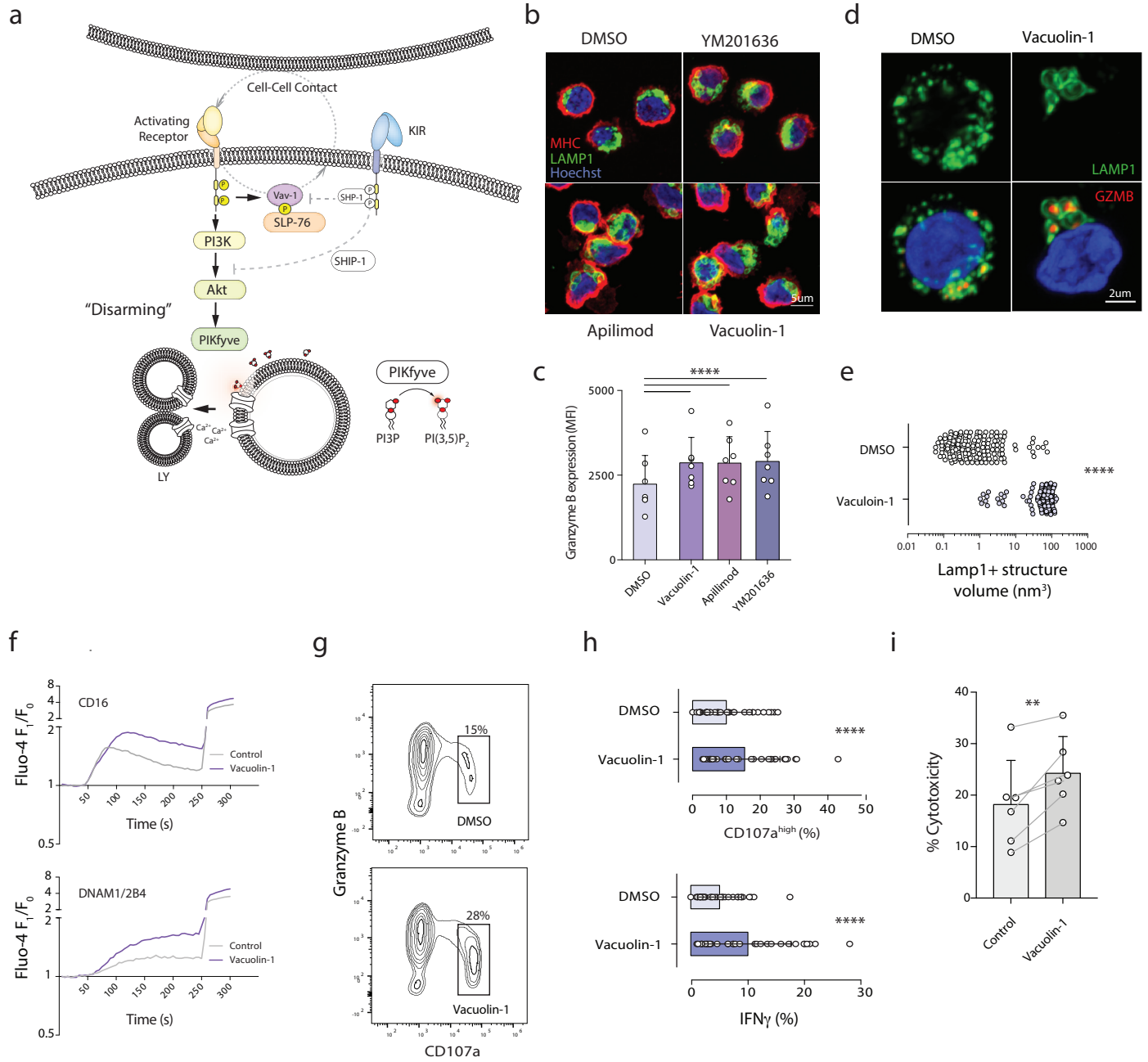
a
Cell-Cell Contact
Activating Receptor
KIR
Vav-1
SLP-76
SHP-1
PI3K
SHIP-1
Akt
"Disarming"
PIKfyve
LY
PI3P
PI(3,5)P2
b
DMSO
YM201636
MHC
LAMP1
Hoechst
5um
Apilimod
Vacuolin-1
d
DMSO
Vacuolin-1
LAMP1
GZMB
2um
c
****
Granzyme B expression (MFI)
5000
2500
0
DMSO
Vacuolin-1
Apilimod
YM201636
e
DMSO
Vacuolin-1
****
0.01
0.1
1
10
100
1000
Lamp1+ structure volume (nm³)
f
CD16
Fluo-4 F1/F0
Control
Vacuolin-1
Time (s)
DNAM1/2B4
g
15%
DMSO
28%
Vacuolin-1
Granzyme B
CD107a
h
DMSO
Vacuolin-1
****
CD107a^high (%)
IFNγ (%)
i
**
% Cytotoxicity
Control
Vacuolin-1
j
p-Zap70/Syk
p-LCK
p-MAPK
p-NF-κB
MFI ratio
No Stim
CD16
CD16 + GPN
CD16 + Vacuolin-1

Figure 6. Pharmacological inhibition of PIKfyve leads to formation of large secretory granules and enhanced NK cell function. (a) Model describing the pathway downstream of activating receptors leading to activation of PIKfyve and TRPML1, lysosomal fission and a hyporesponsive state. Self-specific inhibitory KIRs interfere with activation signals at a proximal level and allow accumulation of dense core granules. (b) Confocal Z-stack showing MHC-I, LAMP-1 and granzyme B (GZMB) staining in primary NK cells following PIKfyve inhibition using overnight incubation with 1μM vacuolin-1, 1μM Apillimod or 1μM YM201636. (c) Intracellular granzyme B expression following incubation with the indicated PIKfyve inhibitor assessed by flow cytometry (n=7). (d) Representative example of confocal image of primary NK cells treated with vacuolin-1 or DMSO. (e) Compiled confocal data on the volume of LAMP-1+ structures from cells treated with DMSO or vacuolin-1 (n=149). (f) Ca^{2+}-flux in NK cells in response to stimulation with biotinylated CD16 (top) or DNAM-/2B4 (bottom) crosslinked with streptavidin in the presence of 10uM vacuolin-1. (g) Representative FACS histogram of granzyme B versus degranulation following stimulation with K562 in the presence of DMSO or 10μM vacuolin-1. (h) Frequency of $CD107a^{high}$+ (top) and IFN-γ+ N K cells (bottom) after stimulation with K562 in the presence of DMSO or 10μM vacuolin-1. (i) FACS-based killing assay showing NK cell killing of K562 cells after treatment with DMSO or 10μM vaculin-1 (n=6) (j) Relative phosphorylation of the indicated signaling molecules following stimulation with biotinylated anti-CD16 (10ug/mL) crosslinked with avidin in the presence of 50μM GPN or 10μM vacuolin-1.

Lysosomal fission is dependent on Ca^{2+} release via the lysosome-specific channel, transient receptor potential mucolipin-1 (TRPML1),[46, 47, 48] which is activated by phosphoinositide 3,5-bisphosphate $PI(3,5)P_2$.[49] $PI(3,5)P_2$ is a downstream derivative of PI3P generated by the PI3P 5-kinase PIKfyve[50] (outlined in Fig. 6a) involved in endosomal maturation and subsequent lysosomal recruitment and degradation. Hence it is well established that PIKfyve is activated downstream of the phosphatidylinositol 3-kinase (PI3K)/AKT pathway.[51] we speculated that unopposed signaling from activating NK cell receptors may modulate the lysosomal compartment through constitutive activation of the PI3K/AKT/PIKfyve pathway. In support of this model, we found that pharmacological inhibition of PIKfyve in resting NK cells by three different small chemical inhibitors: vacuolin-1, apilimod and YM201636,[50] led to enlargement of the lysosomal compartment (Fig. 6b), accompanied by increased levels of granzyme B (Fig. 6c). Confocal microscopy of vacuolin-1 treated primary NK cells revealed localization of granzyme B within enlarged $LAMP\text{-}1^+$ structures (Fig. 6d-e). Treatment of NK cells with vacuolin-1 increased global Ca^{2+} flux in response to receptor-ligation (Fig. 6f) and enhanced specific degranulation (and mobilization of granzyme B) and IFNγ production in response to stimulation by K562 cells (Fig. 6g-h). Furthermore, the increased granzyme B expression and degranulation following PIKfyve inhibition correlated with increased natural cytotoxicity against K562 cells (Fig. 6i). These results demonstrate that chemical blockade of PIKfyve results in enlargement of the granular compartment and enhanced NK cell functionality. In order to identify the point at which lysosomal disruption (GPN) or lysosomal enlargement (vacuolin-1) interfered with intracellular signaling pathways in NK cells, we probed signaling both proximal and distal to the plasma membrane. Vacuolin-1 had a minimal effect on upstream signaling, including ZAP70 and Lck following ligation of CD16 (Fig. 6j). However, the propagation of down-stream signals through NF-κB was increased by treatment with vacuolin-1. Conversely, disruption of lysosomal Ca^{2+}-flux by GPN had the reverse effect on CD16-induced NF-κB signaling (Fig. 6j). Hence, physical modulation of the acidic Ca^{2+} stores affects downstream signaling in response to receptor ligation and tunes NK cell effector responses.

TRPML1-mediated modulation of secretory granules in NK cells PIKfyve is recruited to PI3P positive compartments where it activates the lysosomal Ca^{2+} channel TRPML1 via the production of $PI(3,5)P_2$.[47, 48] Analysis of the transcriptional levels of TRPML1 in discrete NK cell subsets revealed TRPML1 mRNA was expressed at equal levels in all NK cell subset (Fig. 7a). Agonistic stimulation of TRPML using the chemical compound MK6-83, which activates TRPML1 and TRPML3,[52, 53, 54] resulted in loss of granzyme B (Fig. 7b) and decreased specific degranulation and IFNγ responses to K562 cells (Fig. 7c). TRPML3 mRNA was not expressed in resting human NK cells (Data not shown). Conversely, silencing of TRPML1 by siRNA in resting primary NK cells led to increased levels of granzyme B (Fig. 7d-e). Moreover, in concordance with the effects of pharmacological inhibition of PIKfyve, siRNA silencing of TRPML1 (Fig. 7f) led to enhanced degranulation and IFNγ production in primary resting NK cells (Fig. 7g). These results demonstrate a role for TRPML1 in the modulation of granzyme B content and in tuning of effector function in NK cells.

DISCUSSION NK cell education is a dynamic process during which NK cells calibrate their functional

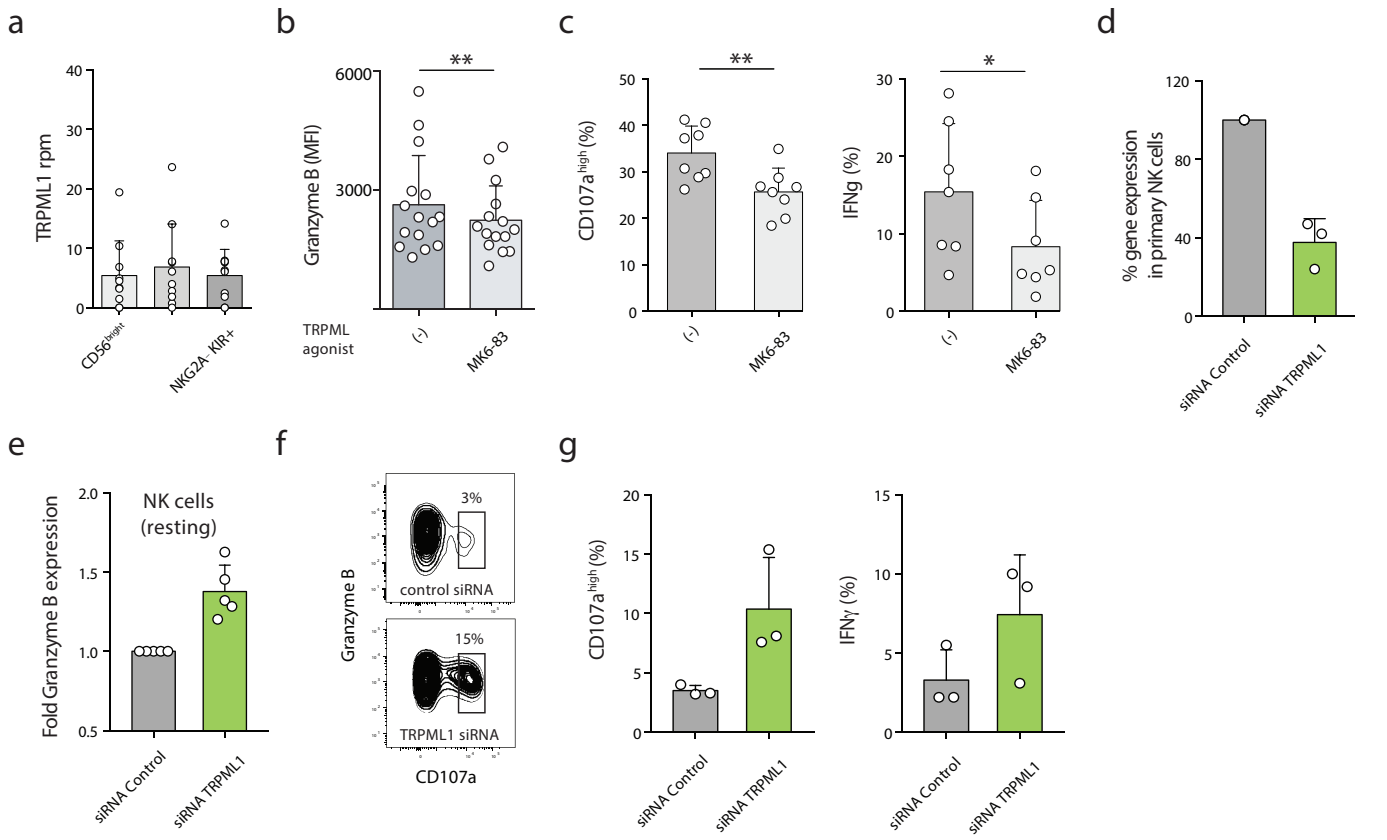

Figure 7. TRPML1-mediated modulation of secretory granules in NK cells (a) mRNA expression (RNA-Seq) of TRPML1 in the indicated NK cell subsets. (b) Granzyme B expression in NK cells treated with 10μM of the TRPML1 agonist MK6-83. (c) Degranulation (left) and IFNγ responses (right) by resting primary NK cells following stimulation with K562 cells in the presence or absence of 10μM MK6-83. (d) Relative mRNA expression (qPCR) of TRPML1 after siRNA silencing in resting NK cells. (e) Relative granzyme B expression after siRNA silencing of TRPML1 in resting NK cells. (f) Representative example of FACS plot showing granzyme B expression versus CD107a^{high} in siRNA TRPML1 silenced primary NK cells after stimulation with K562 cells. (g) Compiled data on degranulation and IFNγ production in TRPML1-silenced primary NK cells. Data are from two independent experiments and three donors with confirmed siRNA silencing.

potential to self-MHC. However, it has been unclear how receptor input during NK cell education is integrated and retained in order for NK cells to remain self-tolerant, whilst also able to deliver spontaneous, well-tuned functional responses upon subsequent challenges. Our results suggest that unopposed activation signals lead to physical disarming of NK cells through TRPML1-induced modulation of the granular compartment. The accumulation of dense-core secretory granules under the influence of inhibitory self-MHC interactions provides mechanistic insights into the paradox of how inhibitory signaling is translated into a state of enhanced functional potential that persists between successive cell-to-cell contacts. A variety of models and nomenclature have been used to describe the process of NK cell education . However, regardless of whether the functional phenotype is caused by gain of function (arming/stimulatory licensing) in self-KIR+ NK cells or loss of function (e.g. disarming/inhibitory licensing) in nonself-KIR+ NK cells,[3, 55] the net outcome of these processes is a consistent difference in the intrinsic functional potential of cells carrying self- and non-self receptors at rest. A structural basis for the difference in functional responsiveness has recently been proposed,[9, 10] whereby educated NK cells display a unique compartmentalization of activating and inhibitory receptors at the nano-scale level on the plasma membrane. Complementing this pre-existing phenotype, we show that NK cell education is also tightly linked to the accumulation of large, granzyme B-rich dense-core cytotoxic granules, located closer to the centrosome in resting NK cells. While the accumulation of dense-core granules, and their specific release during the effector phase, hold important clues to the basis for the increased cytotoxic potential of self-KIR+ NK cells, several outstanding questions remained to be addressed. First, it remained unclear whether the observed accu-

mulation of dense-core granules in self-KIR+ NK cells also contributed to the globally enhanced responsiveness associated with NK cell education.[56] An increasing body of evidence supports the role of the acidic compartment not only in the triggering of Ca^{2+} signaling, but also in the spatiotemporal coordination of signaling cascades[57, 58, 59, 60] and the regulation of receptor degradation.[51] In both T cells and NK cells, lysosomal Ca^{2+} release plays an important role in degranulation.[37, 57] Signaling from the lysosomal compartment was also recently shown to regulate the migratory behavior of dendritic cells in a TRPML1-dependent fashion.[61] Our data suggest that there is a quantitative relationship between modulation of the granular compartment under the influence of inhibitory receptors and intrinsic functional potential of NK cells. While the exact role of the acidic Ca^{2+} store for the enhanced functional potential in self-KIR+ NK cells remains elusive, pharmacological inhibition of Ca^{2+} release from the intracellular acidic stores, together with analysis of Ca^{2+}-flux, consistently pointed to a role for the secretory granule in propagating surface receptor signaling. Notably, a correlation between the size of the lysosomes and level of Ca^{2+}-flux has previously been describe in fibroblasts from patients with Parkinson disease.[62] On that note, it is tempting to speculate that the gain of natural cytotoxicity in lL15 stimulated $CD56^{bright}$ NK cells may be likewise related to the associated enlargement of the granular compartment.[63] Second, we examined the molecular pathway that led to accumulation of dense-core granules in self-KIR positive NK cells, or rather the lack of accumulation of such granules in hyporesponsive NK cells. The difference in granule size and densities in the absence of active lysosomal biogenesis, led us to explore the pathways involved in the continuous modulation of the lysosomal compartment through fission and fusion events 45. Several activating receptors have been implicated in NK cell education, including NKG2D, SLAM family receptors and DNAM-1.[6, 11, 64] NKG2D and DNAM-1 signaling activates the PI3K/AKT pathway.[65, 66] Engagement of inhibitory receptors and SHP-1 signaling block NK cell activation at an early stage of the activation signaling pathway, preventing actin cytoskeleton rearrangement and the recruitment and phosphorylation of activation receptors.[67, 68, 69] The PI3K/AKT pathway is also controlled by SHIP1, which has also been implicated in tuning the effector function of NK cells during education.[70, 71] Notably, PIKfyve and TRPML1 are activated downstream of the PI3K/AKT pathway.[51] Mutations in TRPML1 cause mucolipidosis type IV, which is characterized by enlarged lysosomes.[72, 73] We hypothesized that continuous unopposed signaling through activating receptors during homeostatic cell-cell interactions may trigger the AKT/PIKfyve/TRPML1 axis and thereby promote lysosomal fission, leading to an inability to accumulate dense-core granules. To explore this hypothesis, we used a combination of pharmacological agonists and antagonists combined with genetic approaches to interfere with the PIKfyve/TRPML1 pathway. Pharmacological inhibition of PIKfyve by small chemical compounds, including vacuolin-1 and apilimod is known to cause enlarged lysosomes in several cell types, including mast cells and macrophages.[50, 74, 75] Here, we show that inhibition of PIKfyve by three different chemical compounds caused enlargement of the lysosomal compartment. Importantly, this was associated with increased granzyme B expression, increased Ca^{2+}-flux, and more potent effector function. A similar functional phenotype was obtained when silencing the lysosome-specific Ca^{2+} release channel TRPML1. Together these data support a model where tonic or intermittent activation signals through the PI3K/AKT pathway result in PIKfyve activation and TRPML1-induced lysosomal fission, ultimately leading to lack of dense-core granules and reduced functional potential in NK cells. In Chediak-Higashi Syndrome (CHS), mutation of the LYST gene leads to the formation of giant secretory lysosomal structures.[76] NK cells in CHS patients are hyperresponsive and hypersecretory but are unable to degranulate.[77, 78] Although NK cell activation followed by granule convergence and polarization appears to be normal in LYST-deficient NK cells, the enlarged granules fail to pass through the cortical actin meshwork openings at the immunological synapse.[36] By monitoring granule size and granzyme B density prior to and following degranulation, we observed a selective loss of the pre-converged, large dense-core granules after degranulation. These large granules had an area above 0,2 μm^2, corresponding to a diameter of around 500nm, pointing to a possible difference in the density of the actin meshwork and physical restriction of degranulation between resting primary NK cells and NK92 cells. However, another contributing

factor may be LYST-mediated modulation of granules during during the effector response allowing smaller proportions of the large granules to be released, as has been demonstrated for degranulation in mast cells.[79] An outstanding question is how lysosomal fission leads to loss of the granular matrix and granzyme B in hyporesponsive NK cells. Granzyme B can be synthesized and secreted directly through the constitutive secretory pathway.[80] It is possible that an enhanced rate of lysosomal fission during weakly agonistic cell-cell interactions and the corresponding failure to accumulate dense-core granules in NK cells lacking self-specific receptors leads to loss of granzyme through the secretory route.[81] Indeed, NK cells in serglycin$^{-/-}$ mice lack dense-core granules, retain less granzyme B which is secreted from the cell at a greater rate, and exhibit reduced degranulation in response to stimuli.[34] Another remaining challenge is to decipher when and where TRPML1-mediated physical disarming takes place. Transfer experiments in mice have established an indisputable role for cell-to-cell interactions in shaping the functionality of mature NK cells.[82, 83, 84] Although the detailed time-scale and spatial aspects of such cell interactions remain largely unknown, transfer of functional NK cells to MHC-deficient environments leads to induction of hyporesponsiveness.[4] SHP-1 intersects signaling of activating receptors upstream of Vav-1[69] and rapidly shuts down the process of forming an activating NK cell synapse with target cells.[85] While the inhibitory synapse and the productive cytolytic synapse have been studied in great detail, much less is known about immune synapses formed between resting immune cells during homeostasis. It is possible that cells lacking self-specific inhibitory receptors form a succession of non-cytolytic immune synapses under homeostasis leading to loss of dense-core granules and "leakage" of their functional potential.[81] It has previously been shown that trans-presentation of IL-15 to NK cells, resulting in activation of AKT is negatively regulated by inhibitory interactions with self MHC.[86] Thus, it is possible that unopposed constitutive IL-15 activation may occur in NK cells that lack self-specific inhibitory KIR, which in turn would affect granular stability and/or retention through the mechanism described here. The dose dependant induction of granzyme B expression in response to cytokine, or viral infection, is connected to activation of the metabolic checkpoint kinase mTOR.[19] Notably, however, we did not observe any transcriptional imprint in the mTOR pathway when we examined circulating NK cells at rest, arguing against a major role for metabolism in the persistence of the unique granular phenotype seen in circulating blood self-KIR+ NK cells. It was recently shown that mTOR activation contributed to the functional rheostat during effector responses in educated murine NK cells.[87] Interestingly, mTOR activation and function are dependent on its lysosomal localization and the vacuolar H(+) -ATPase (V-ATPase) activity.[88] Thus, the difference in lysosomal composition described in the present study could potentially contribute to enhanced mTOR activation observed in educated NK cells upon stimulation.[87] In conclusion, our findings suggest a mechanism by which NK cell education operates through modulation of dense-core granules under the influence of inhibitory receptor ligand interactions. Qualitative differences in the morphology of the lysosomal compartment and signaling from acidic Ca^{2+} stores, allow the cytolytic machinery to operate independently of transcription during the effector response. Furthermore, the data suggest that it may be possible to boost NK cell functionality through targeted manipulation of the granular matrix and Ca^{2+} homeostasis within lysosome-related organelles.

METHODS

Cells

Buffy coats from random healthy blood donors were obtained from the Karolinska University Hospital and Oslo University Hospital Blood banks with informed consent. Peripheral blood mononuclear cells were separated from buffy coats by density gravity centrifugation (Lymphoprep; Axis-Shield) using fretted spin tubes (Sepmate; Stemcell Technologies). Genomic DNA was isolated from 200µl of whole blood using DNeasy Blood and Tissue Kit (Qiagen). KIR ligands were determined using the KIR HLA ligand kit (Olerup SSP) for detection of the HLA-Bw4, HLA-C1, and HLA-C2 motifs. NK cells were purified using negative selection (Miltenyi) with an AutoMACS Pro Seperator. K562 cells were maintained in RPMI +10%FCS.

Phenotyping by Flow Cytometry

Isolated PBMC were stained for flow cytometric analysis using an appropriate combination of antibodies

as detailed in the supplementary experimental procedures. After surface staining, cells were fixed and permeabilized using a fixation/permeabilization kit (BD Bioscience Cytofix/Cytoperm) prior to intracellular staining with anti-granzyme B-A700 (GB11). Samples were acquired using an LSRII flow cytometer (Becton Dickinson) and data was analyzed using FlowJo V10.0.8 (TreeStar). Stochastic neighbor embedding (SNE) analysis was performed as described in supplementary experimental procedures

RNAseq and qPCR

RNASeq was performed using single-cell tagged reverse transcription (STRT), a highly multiplexed method for single-cell RNA-seq. Real time quantitative PCR was used to study the difference in the expression of 20 genes of interest in sorted differentiation and education subsets of NK cells, as detailed in supplementary experimental procedures.

Confocal fluorescence microscopy and Image analysis

Staining and preparation of cells for confocal microscopy is detailed in supplementary experimental procedures. The cells were examined with a Zeiss LSM 710 confocal microscope (Carl Zeiss MicroImaging GmbH) equipped with an Ar-Laser Multiline (458/488/514nm), a DPSS-561 10 (561nm), a Laser diode 405-30 CW (405nm), and a HeNe-laser (633nm). The objective used was a Zeiss plan-Apochromat 63xNA/1.4 oil DICII. Image processing and analysis were performed with basic software ZEN 2011 (Carl Zeiss MicroImaging GmbH) and Imaris 7.7.2 (Bitplane AG). Confocal z-stacks were deconvolved using Huygens Essential 14.06 (Scientific Volume Imaging b.v.), and visualized with Imaris.

Electron Microscopy

Preparation of cells for electron microscopy is detailed in supplementary experimental procedures. Ultrathin sections (70-90 nm) of cell pellets were cut on a Leica Ultracut (equipped with UFC cryochamber) at -110C, picked up with a 50:50 mixture of 2.3 M sucrose and 2% methyl cellulose. Sections were then labeled with antibodies against granzyme B (496B, eBioscience) or Chondroitin Sulphate 4 (2B6, AMSBIO), followed by a bridging rabbit-anti-mouse antibody (DAKO, Denmark) and protein A gold (University Medical Center, Utrecht, Netherlands). Microscopy was done at 80 kV in a JEOL_JEM1230 and images acquired with a Morada camera. Further image processing was done in Adobe Photoshop. Quantification was done according to established stereological procedures.

Functional Assays

Standard cell based functional assays, calcium flux assays and phospho flow cytometry are detailed in supplementary experimental procedures. Treatment with lysosomotropic reagents were performed for the duration of the assay using the following final concentrations; Glycyl-L-Phenylalanine-β-Naphthylamide (GPN, 50uM), mefloquine (10μM), vacuolin-1 (1-10μM). The TRPML1/3 agonist MK6-83 was used at 10μM.

Ca^{2+} Flux Assay

Freshly isolated NK cells were incubated with Fluo-4 for 30 min at 37C in PBS+2%FCS at the recommended dilution (Fluo-4 Imaging kit, Molecular Probes). Cells were then washed twice and incubated with biotinylated CD16 or biotinylated DNAM-1/2B4 (Miltenyi), with the addition of labeled specific antibodies for CD56, CD57, NKG2A, KIR2DL1, KIR2DL1/S1, KIR3DL1/S1 and KIR2DL2/L3/S2, for 10 min at room temperature. The cells were washed once more and placed on ice until assayed. Prior to FACS analysis, the cells were pre-warmed at 37C for 5 min in the presence or absence of GPN (50μM final concentration) or vacuolin-1 (10μM final concentration). Cells were immediately run on FACS for 30s, followed by addition of 10ug/mL Streptavidin and run for a further 4 min. Ionomycin was added at 4μM final concentration and run for a further 1 min. Ca^{2+}-flux kinetics were analysed by FlowJo V10.0.8 (TreeStar).

siRNA Interference

Primary NK cells were isolated, rested for 2 hours and transfected either directly or Primed with 10ng/mL IL15 for 72 hours and transfected. NK cells or cell lines were transfected by Amaxa nucleofection (Lonza) using 300pM of Dharmacon ON-TARGET plus SMARTpool control siRNA, or SMARTpool RNA targeting human TRPML1. Nuclefection was performed using the human macrophage kit using program Y-010. After nucleofection, cells were rested for 4 hours in OPTI-MEM, before an equal volume

of culture medium with 2ng/ml IL15 was added. The cells were then cultured for 48 hours before phenotypic and functional testing. siRNA efficiency was determined using qPCR.

Statistical analysis

Comparisons of matched groups were made using paired Students T test. Single comparison of groups or populations of cells between donors was performed using Students t test or Mann-Whitney test for statistical significance. n.s. indicates not significant; ****$p < 0.0001$***; $p < 0.001$; **$p < 0.01$; and *$p < 0.05$. Analyses were performed using GraphPad Prism software.

AUTHOR CONTRIBUTION

JPG designed and performed research, analysed data and wrote the paper. BJ, DC, ES and AB performed imaging experiments and analysed data. LM-Z, SL, TC, UK, SL and MLS performed RNA Seq and qPCR and analysed data. WEL contributed to the Ca-signaling experiments. JL performed Phospho-flow experiments. AP, MTW, EH A, LL and VSO performed experiments. SP, CG, KT and HS contributed to the design of research and the writing of the paper. KJM designed research, analysed data and wrote the paper.

ACKNOWLEDGEMENT

This work was supported by grants from the Swedish Research Council, the Swedish Children's Cancer Society, the Swedish Cancer Society, the Tobias Foundation, the Karolinska Institutet, the Wenner-Gren Foundation, the Norwegian Cancer Society, the Norwegian Research Council, the South-Eastern Norway Regional Health Authority and the KG Jebsen Center for Cancer Immunotherapy. SP was supported by BB/N01524X/1 from the BBSRC and BJ was funded by a Mildred Scheel postdoctoral scholarship from the Dr. Mildred Scheel Foundation for Cancer Research of the German Cancer Aid Organization.

REFERENCES

1. Karre, K., Ljunggren, H.G., Piontek, G. & Kiessling, R. Selective rejection of H-2-deficient lymphoma variants suggests alternative immune defence strategy. Nature 319, 675-678 (1986).
2. Anfossi, N. et al. Human NK cell education by inhibitory receptors for MHC class I. Immunity 25, 331-342 (2006).
3. Elliott, J.M. & Yokoyama, W.M. Unifying concepts of MHC-dependent natural killer cell education. Trends Immunol 32, 364-372 (2011).
4. Joncker, N.T., Shifrin, N., Delebecque, F. & Raulet, D.H. Mature natural killer cells reset their responsiveness when exposed to an altered MHC environment. J Exp Med 207, 2065-2072 (2010).
5. Elliott, J.M., Wahle, J.A. & Yokoyama, W.M. MHC class I-deficient natural killer cells acquire a licensed phenotype after transfer into an MHC class I-sufficient environment. J Exp Med 207, 2073-2079 (2010).
6. Chen, S. et al. The Self-Specific Activation Receptor SLAM Family Is Critical for NK Cell Education. Immunity 45, 292-304 (2016).
7. Kim, S. et al. Licensing of natural killer cells by host major histocompatibility complex class I molecules. Nature 436, 709-713 (2005).
8. Viant, C. et al. SHP-1-mediated inhibitory signals promote responsiveness and anti-tumour functions of natural killer cells. Nat Commun 5, 5108 (2014).
9. Guia, S. et al. Confinement of activating receptors at the plasma membrane controls natural killer cell tolerance. Science signaling 4, ra21 (2011).
10. Staaf, E. et al. Educated natural killer cells show dynamic movement of the activating receptor NKp46 and confinement of the inhibitory receptor Ly49A. Science signaling 11 (2018).
11. Enqvist, M. et al. Coordinated Expression of DNAM-1 and LFA-1 in Educated NK Cells. J Immunol 194, 4518-4527 (2015).
12. van Bergen, J. et al. HLA reduces killer cell Ig-like receptor expression level and frequency in a humanized mouse model. J Immunol 190, 2880-2885 (2013).
13. Boudreau, J.E. & Hsu, K.C. Natural killer cell education in human health and disease. Curr Opin Immunol 50, 102-111 (2018).
14. Brodin, P. & Hoglund, P. Beyond licensing and disarming: a quantitative view on NK-cell education. Eur J Immunol 38, 2934-2937 (2008).
15. Fehniger, T.A. et al. Acquisition of murine NK cell cytotoxicity requires the translation of a pre-existing pool of granzyme B and perforin mRNAs. Immunity 26, 798-811 (2007).
16. Huntington, N.D. et al. IL-15 trans-presentation promotes human NK cell development and differentiation in vivo. J Exp Med 206, 25-34 (2009).
17. McDougall, I.R. & Rieser, R.P. Scintigraphic techniques in musculoskeletal trauma. Radiol Clin North Am 27, 1003-1011 (1989).
18. Donnelly, R.P. et al. mTORC1-dependent metabolic reprogramming is a prerequisite for NK cell effector function. J Immunol 193, 4477-4484 (2014).
19. Marcais, A. et al. The metabolic checkpoint kinase mTOR is essential for IL-15 signaling during the development and activation of NK cells. Nat Immunol 15, 749-757 (2014).
20. Boysen, P., Eide, D.M. & Storset, A.K. Natural killer cells in free-living Mus musculus have a primed phenotype. Mol Ecol 20, 5103-5110 (2011).
21. Lopez-Verges, S. et al. CD57 defines a functionally distinct population of mature NK cells in the human CD56dimCD16+ NK-cell subset. Blood 116, 3865-3874 (2010).
22. Bjorkstrom, N.K. et al. Expression patterns of NKG2A, KIR, and CD57 define a process of CD56dim NK-cell differentiation uncoupled from NK-cell education. Blood 116, 3853-3864 (2010).
23. Valiante, N.M. et al. Functionally and structurally distinct NK cell receptor repertoires in the peripheral blood of two human donors. Immunity 7, 739-751 (1997).
24. Andersson, S., Fauriat, C., Malmberg, J.A., Ljunggren, H.G. & Malmberg, K.J. KIR acquisition probabilities are independent of self-HLA class I ligands and increase with cellular KIR expression. Blood 114, 95-104 (2009).
25. Boudreau, J.E., Mulrooney, T.J., Le Luduec, J.B., Barker, E. & Hsu, K.C. KIR3DL1 and HLA-B Density and Binding Calibrate NK Education and Response to HIV. J Immunol 196, 3398-3410 (2016).
26. Fauriat, C. et al. Estimation of the size of the alloreactive NK cell repertoire: studies in individuals homozygous for the group A KIR haplotype. J Immunol 181, 6010-6019 (2008).

27. Yawata, M. et al. MHC class I-specific inhibitory receptors and their ligands structure diverse human NK-cell repertoires toward a balance of missing self-response. Blood 112, 2369-2380 (2008).
28. Yu, J. et al. Hierarchy of the human natural killer cell response is determined by class and quantity of inhibitory receptors for self-HLA-B and HLA-C ligands. J Immunol 179, 5977-5989 (2007).
29. Islam, S. et al. Highly multiplexed and strand-specific single-cell RNA 5' end sequencing. Nat Protoc 7, 813-828 (2012).
30. Kallies, A. et al. A role for Blimp1 in the transcriptional network controlling natural killer cell maturation. Blood 117, 1869-1879 (2011).
31. Kurachi, M. et al. The transcription factor BATF operates as an essential differentiation checkpoint in early effector CD8+ T cells. Nat Immunol 15, 373-383 (2014).
32. Man, K. et al. The transcription factor IRF4 is essential for TCR affinity-mediated metabolic programming and clonal expansion of T cells. Nat Immunol 14, 1155-1165 (2013).
33. Luetke-Eversloh, M. et al. NK cells gain higher IFN-gamma competence during terminal differentiation. Eur J Immunol 44, 2074-2084 (2014).
34. Sutton, V.R. et al. Serglycin determines secretory granule repertoire and regulates natural killer cell and cytotoxic T lymphocyte cytotoxicity. FEBS J 283, 947-961 (2016).
35. Kolset, S.O. & Pejler, G. Serglycin: a structural and functional chameleon with wide impact on immune cells. J Immunol 187, 4927-4933 (2011).
36. Gil-Krzewska, A. et al. An actin cytoskeletal barrier inhibits lytic granule release from Natural Killer cells in Chediak-Higashi syndrome. J Allergy Clin Immunol (2017).
37. Speak, A.O. et al. Altered distribution and function of natural killer cells in murine and human Niemann-Pick disease type C1. Blood 123, 51-60 (2014).
38. Pores-Fernando, A.T. & Zweifach, A. Calcium influx and signaling in cytotoxic T-lymphocyte lytic granule exocytosis. Immunol Rev 231, 160-173 (2009).
39. Penny, C.J., Kilpatrick, B.S., Han, J.M., Sneyd, J. & Patel, S. A computational model of lysosome-ER Ca2+ microdomains. J Cell Sci 127, 2934-2943 (2014).
40. Jadot, M., Colmant, C., Wattiaux-De Coninck, S. & Wattiaux, R. Intralysosomal hydrolysis of glycyl-L-phenylalanine 2-naphthylamide. Biochem J 219, 965-970 (1984).
41. Sukhai, M.A. et al. Lysosomal disruption preferentially targets acute myeloid leukemia cells and progenitors. J Clin Invest 123, 315-328 (2013).
42. Paivandy, A. et al. Mefloquine, an anti-malaria agent, causes reactive oxygen species-dependent cell death in mast cells via a secretory granule-mediated pathway. Pharmacol Res Perspect 2, e00066 (2014).
43. Lloyd-Evans, E. et al. Niemann-Pick disease type C1 is a sphingosine storage disease that causes deregulation of lysosomal calcium. Nat Med 14, 1247-1255 (2008).
44. Saftig, P. & Klumperman, J. Lysosome biogenesis and lysosomal membrane proteins: trafficking meets function. Nature reviews. Molecular cell biology 10, 623-635 (2009).
45. Luzio, J.P., Pryor, P.R. & Bright, N.A. Lysosomes: fusion and function. Nature reviews. Molecular cell biology 8, 622-632 (2007).
46. Cao, Q., Yang, Y., Zhong, X.Z. & Dong, X.P. The lysosomal Ca(2+) release channel TRPML1 regulates lysosome size by activating calmodulin. J Biol Chem 292, 8424-8435 (2017).
47. Pryor, P.R., Reimann, F., Gribble, F.M. & Luzio, J.P. Mucolipin-1 is a lysosomal membrane protein required for intracellular lactosylceramide traffic. Traffic 7, 1388-1398 (2006).
48. Thompson, E.G., Schaheen, L., Dang, H. & Fares, H. Lysosomal trafficking functions of mucolipin-1 in murine macrophages. BMC Cell Biol 8, 54 (2007).
49. Dong, X.P. et al. PI(3,5)P(2) controls membrane trafficking by direct activation of mucolipin Ca(2+) release channels in the endolysosome. Nat Commun 1, 38 (2010).
50. Sano, O. et al. Vacuolin-1 inhibits autophagy by impairing lysosomal maturation via PIKfyve inhibition. FEBS Lett 590, 1576-1585 (2016).
51. Er, E.E., Mendoza, M.C., Mackey, A.M., Rameh, L.E. & Blenis, J. AKT facilitates EGFR trafficking and degradation by phosphorylating and activating PIKfyve. Science signaling 6, ra45 (2013).
52. Grimm, C., Bartel, K., Vollmar, A.M. & Biel, M. Endolysosomal Cation Channels and Cancer-A Link with Great Potential. Pharmaceuticals (Basel) 11 (2018).
53. Chen, C.C. et al. A small molecule restores function to TRPML1 mutant isoforms responsible for mucolipidosis type IV. Nat Commun 5, 4681 (2014).
54. Shen, D. et al. Lipid storage disorders block lysosomal trafficking by inhibiting a TRP channel and lysosomal calcium release. Nat Commun 3, 731 (2012).
55. Raulet, D.H. & Vance, R.E. Self-tolerance of natural killer cells. Nat Rev Immunol 6, 520-531 (2006).
56. Hoglund, P. & Brodin, P. Current perspectives of natural killer cell education by MHC class I molecules. Nat Rev Immunol (2010).
57. Davis, L.C. et al. NAADP activates two-pore channels on T cell cytolytic granules to stimulate exocytosis and killing. Curr Biol 22, 2331-2337 (2012).
58. Patel, S. & Docampo, R. Acidic calcium stores open for business: expanding the potential for intracellular Ca2+ signaling. Trends Cell Biol 20, 277-286 (2010).
59. Patel, S. & Cai, X. Evolution of acidic Ca(2)(+) stores and their resident Ca(2)(+)-permeable channels. Cell Calcium 57, 222-230 (2015).
60. Wolf, I.M. et al. Frontrunners of T cell activation: Initial, localized Ca2+ signals mediated by NAADP and the type 1 ryanodine receptor. Sci Signal 8, ra102 (2015).
61. Bretou, M. et al. Lysosome signaling controls the migration of dendritic cells. Sci Immunol 2 (2017).
62. Hockey, L.N. et al. Dysregulation of lysosomal morphology by pathogenic LRRK2 is corrected by TPC2 inhibition. J Cell Sci 128, 232-238 (2015).
63. Wagner, J.A. et al. CD56bright NK cells exhibit potent antitumor responses following IL-15 priming. J Clin Invest 127, 4042-4058 (2017).
64. Thompson, T.W. et al. Endothelial cells express NKG2D ligands and desensitize anti-tumor NK responses. Elife 6 (2017).
65. Kwon, H.J. et al. Stepwise phosphorylation of p65 promotes NF-kappaB activation and NK cell responses during target cell recognition. Nat Commun 7, 11686 (2016).
66. Upshaw, J.L. et al. NKG2D-mediated signaling requires a DAP10-bound Grb2-Vav1 intermediate and phosphatidylinositol-3-kinase in human natural killer cells. Nat Immunol 7, 524-532 (2006).
67. Lodeiro, M. et al. The SHP-1 protein tyrosine phosphatase negatively modulates Akt signaling in the ghrelin/GHSR1a system. Mol Biol Cell 22, 4182-4191 (2011).
68. Bryceson, Y.T. & Long, E.O. Line of attack: NK cell specificity and integration of signals. Curr Opin Immunol 20, 344-352 (2008).
69. Stebbins, C.C. et al. Vav1 dephosphorylation by the tyrosine phosphatase SHP-1 as a mechanism for inhibition of cellular cytotoxicity. Mol Cell Biol 23, 6291-6299 (2003).
70. Gumbleton, M. et al. Dual enhancement of T and NK cell function by pulsatile inhibition of SHIP1 improves antitumor immunity and survival. Science signaling 10 (2017).
71. Gumbleton, M., Vivier, E. & Kerr, W.G. SHIP1 intrinsically regulates NK cell signaling and education, resulting in tolerance of an MHC class I-mismatched bone marrow graft in mice. J Immunol 194,

2847-2854 (2015).
72. Chen, C.S., Bach, G. & Pagano, R.E. Abnormal transport along the lysosomal pathway in mucolipidosis, type IV disease. Proc Natl Acad Sci U S A 95, 6373-6378 (1998).
73. Miller, A. et al. Mucolipidosis type IV protein TRPML1-dependent lysosome formation. Traffic 16, 284-297 (2015).
74. Shaik, G.M., Draberova, L., Heneberg, P. & Draber, P. Vacuolin-1-modulated exocytosis and cell resealing in mast cells. Cell Signal 21, 1337-1345 (2009).
75. Choy, C.H. et al. Lysosome enlargement during inhibition of the lipid kinase PIKfyve proceeds through lysosome coalescence. J Cell Sci (2018).
76. Nagle, D.L. et al. Identification and mutation analysis of the complete gene for Chediak-Higashi syndrome. Nat Genet 14, 307-311 (1996).
77. Gil-Krzewska, A. et al. Chediak-Higashi syndrome: Lysosomal trafficking regulator domains regulate exocytosis of lytic granules but not cytokine secretion by natural killer cells. J Allergy Clin Immunol 137, 1165-1177 (2016).
78. Chiang, S.C.C. et al. Differences in Granule Morphology yet Equally Impaired Exocytosis among Cytotoxic T Cells and NK Cells from Chediak-Higashi Syndrome Patients. Frontiers in immunology 8, 426 (2017).
79. Chen, H.Y. et al. Nanoimaging granule dynamics and subcellular structures in activated mast cells using soft X-ray tomography. Sci Rep 6, 34879 (2016).
80. Isaaz, S., Baetz, K., Olsen, K., Podack, E. & Griffiths, G.M. Serial killing by cytotoxic T lymphocytes: T cell receptor triggers degranulation, re-filling of the lytic granules and secretion of lytic proteins via a non-granule pathway. Eur J Immunol 25, 1071-1079 (1995).
81. Goodridge, J.P., Onfelt, B. & Malmberg, K.J. Newtonian cell interactions shape natural killer cell education. Immunol Rev 267, 197-213 (2015).
82. Landtwing, V. et al. Cognate HLA absence in trans diminishes human NK cell education. J Clin Invest (2016).
83. Boudreau, J.E. et al. Cell-Extrinsic MHC Class I Molecule Engagement Augments Human NK Cell Education Programmed by Cell-Intrinsic MHC Class I. Immunity 45, 280-291 (2016).
84. Ebihara, T., Jonsson, A.H. & Yokoyama, W.M. Natural killer cell licensing in mice with inducible expression of MHC class I. Proc Natl Acad Sci U S A 110, E4232-4237 (2013).
85. Orange, J.S. et al. Wiskott-Aldrich syndrome protein is required for NK cell cytotoxicity and colocalizes with actin to NK cell-activating immunologic synapses. Proc Natl Acad Sci U S A 99, 11351-11356 (2002).
86. Anton, O.M., Vielkind, S., Peterson, M.E., Tagaya, Y. & Long, E.O. NK Cell Proliferation Induced by IL-15 Transpresentation Is Negatively Regulated by Inhibitory Receptors. J Immunol 195, 4810-4821 (2015).
87. Marcais, A. et al. High mTOR activity is a hallmark of reactive natural killer cells and amplifies early signaling through activating receptors. Elife 6 (2017).
88. Zoncu, R. et al. mTORC1 senses lysosomal amino acids through an inside-out mechanism that requires the vacuolar H(+)-ATPase. Science 334, 678-683 (2011).